Coherent X-ray Radiation from a Relativistic Electron in a Combined Medium

S. V. Blazhevich and A. V. Noskov*

Belgorod State National Research University, ul. Pobedy 85, Belgorod, 308015 Russia

**e-mail: noskovbupk@mail.ru*

Abstract—A theory of coherent X-ray radiation from a relativistic electron crossing a combined medium that consists of amorphous and crystal plates is constructed within the dynamic diffraction theory. The field reflection asymmetry relative to the target surface determined by the angle between the atomic planes and the target surface is taken into account in the theory. The expressions describing the spectral-angular densities of parametric X-ray and diffracted transition radiations in this medium are derived and investigated.

DOI: 10.1134/S106377611403011X

1. INTRODUCTION

The coherent X-ray radiation of a relativistic electron has always been considered separately in a crystal and an amorphous medium. In an amorphous medium, when it is crossed by a uniformly moving relativistic electron, transition radiation [1, 2] is generated near the electron velocity direction. Despite the fact that it was discovered long ago, the transition radiation is still being investigated for various complex surfaces and under various external conditions [3–8]. The great interest in the transition radiation of relativistic electrons stems primarily from the possibility of using it as an X-ray radiation source [9]. It should be noted that although the transition radiation is intense and narrowly beamed, it has a wide spectral range and intense monochromatic radiation is often needed for applications. When a charged particle crosses the surface of a crystal plate, the transition radiation arising at the boundary is diffracted by a system of parallel atomic planes in the crystal to produce diffracted transition radiation (DTR) [10–13] whose photons move in the Bragg scattering direction in a narrow spectral range. When a fast charged particle crosses a single crystal, its Coulomb field is scattered by a system of parallel atomic planes in the crystal to generate parametric X-ray radiation (PXR) [14–16] whose photons together with the DTR photons move in the Bragg scattering direction. At present, there are two approaches to describe the PXR process: kinematic [17, 18] and dynamic [15, 16, 19]. It should be noted that the diffracted transition radiation by itself is a dynamic effect, namely the dynamic diffraction effect. Note that the kinematic approach takes into account the interactions of each atom only with the primary, or refracted, wave in the crystal. In this approach, in contrast to the dynamic one, the interaction of an atom with the wave field produced in the crystal by the combined scattering by all other atoms is neglected, i.e., the multiwave scattering, in particular, the interaction of elementary waves with the refracted one and the reflections of waves between the atomic planes are disregarded. The coherent X-ray radiation of relativistic electrons in a crystal was developed within the dynamic diffraction theory in [20–25]. It should be noted that the coherent X-ray radiation is considered in [20–22] in the special case of symmetric reflection where the reflecting system of atomic planes in the crystal is parallel and perpendicular to the target surface for the Bragg and Laue scattering geometries, respectively. The dynamic theory of coherent X-ray radiation from relativistic electrons in a crystal was developed in [23–25] in the general case of asymmetric electron field reflection relative to the target surface where the system of parallel reflecting target layers can be oriented at an arbitrary angle to the target surface.

In this paper, the coherent radiation of a relativistic electron crossing a combined medium that consists of amorphous and crystal plates is considered for the first time. We take into account the fact that PXR and DTR in the crystal plate undergo dynamic diffraction under conditions of asymmetric field reflection relative to the target surface, i.e., the system of reflecting atomic planes in the crystal plate is oriented at an arbitrary angle, while considering the Laue scattering geometry. The expressions describing the spectral-angular distributions of PXR and DTR in the structure under consideration are derived within the two-wave approximation of the dynamic diffraction theory. We consider the possibility of increasing the intensity of DTR from a relativistic electron without increasing the electron energy by placing an amorphous plate in front of the crystal plate. Under optimal conditions for PXR generation, one might expect an increase in the source's efficiency precisely through DTR whose intensity can

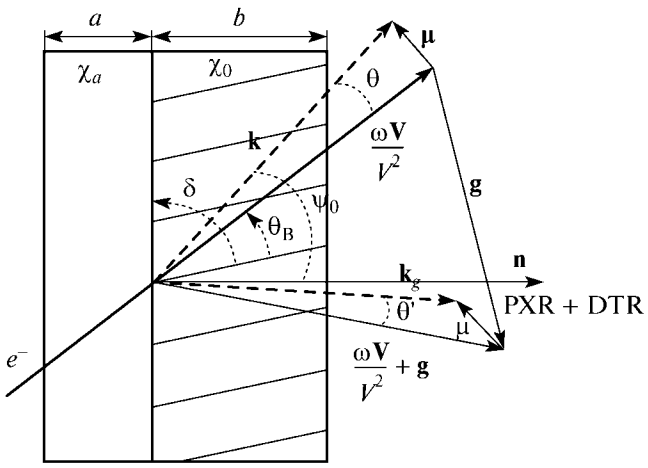

Fig. 1. Radiation geometry and notation: θ and θ' are the radiation angles, θ_B is the Bragg angle (the angle between the electron velocity $\mathbf{V}$ and the atomic planes), δ is the angle between the surface and the atomic planes of the crystal under consideration, $\mathbf{k}$ and $\mathbf{k}_g$ are the wave vectors of the incident and diffracted photons, respectively.

be raised by increasing the number of boundaries at which it is generated. The angular DTR density is shown to increase with amorphous-plate density. This result is interesting from the viewpoint of creating a compact, intense quasi-monochromatic X-ray source. We consider the possibility of using the expressions derived here to interpret the experimental data where the substrate on which a thin crystal plate is located is amorphous.

2. THE RADIATION FIELD AMPLITUDE

Consider a relativistic electron passing with a velocity $\mathbf{V}$ through a combined target that consists of amorphous and crystal plates (see Fig. 1) with thicknesses a and b, respectively. Denote the dielectric susceptibilities of the amorphous medium by χ_a and the crystal medium by χ_0 and χ_g. When the relativistic electron crosses the first (vacuum–amorphous medium) and second (amorphous medium–crystal) target boundaries, transition radiation arises and then is diffracted in the crystal plate by a system of parallel atomic planes in the Bragg scattering direction (in the direction of the wave vector $\mathbf{k}_g = \mathbf{k} + \mathbf{g}$; see Fig. 1) to generate the diffracted transition radiation emerging through the third boundary (crystal–vacuum) together with the parametric X-ray radiation produced in the crystal plate. Constructive or destructive interference between the transition radiation waves excited at the first two target boundaries and contributing to the DTR yield is possible, depending on the parameters of the amorphous layer and the angle of incidence of the electron on the target.

We will consider the propagation of X-ray waves in the crystal medium within the two-wave approximation of the dynamic diffraction theory. In Fig. 1, $\boldsymbol{\mu} = \mathbf{k} - \omega\mathbf{V}/V^2$ is the virtual photon momentum component perpendicular to the particle velocity $\mathbf{V}$ ($\mu = \omega\theta/V$, where $\theta \ll 1$ is the angle between the vectors $\mathbf{k}$ and $\mathbf{V}$), θ_B is the Bragg angle, φ is the azimuthal angle of the radiation propagation measured from the plane formed by the velocity vector $\mathbf{V}$ and the reciprocal lattice vector $\mathbf{g}$ in the crystal. The length of the vector $\mathbf{g}$ can be expressed in terms of the Bragg angle and Bragg frequency ω_B as $g = 2\omega_B \sin\theta_B/V$. We denote the angle between the vector $\omega\mathbf{V}/V^2$ and the wave vector of the incident wave $\mathbf{k}$ by θ and the angle between the vector $\omega\mathbf{V}/V^2 + \mathbf{g}$ and the wave vector of the diffracted wave $\mathbf{k}_g$ by θ'.

In [25], we constructed a theory of coherent X-ray radiation in a direction of the vector $\mathbf{k}$ (see Fig. 1) close to the velocity direction of the relativistic electron crossing the crystal plate, while considering the total radiation as the sum of forward PXR (FPXR) and transition radiation (TR). However, in the two-wave approximation of the dynamic diffraction theory [26], a photon in the direction of $\mathbf{k}_g$ corresponds to each photon in the direction of k. In this paper, the radiations and diffraction of X-ray waves in the crystal plate in the direction of $\mathbf{k}_g$ are described just as in [25, 27]. Using the notation and methods applied in [25, 27], let us write the expressions for the electric fields in a vacuum in the amorphous and crystal plates. In a vacuum in front of the target, the field consists of the pseudo-photons of the relativistic-electron Coulomb field:

$$E_0^{(s)\mathrm{vacl}} = \frac{8\pi^2 ieV\theta P^{(s)}}{\omega} \times \left\{\frac{\gamma_0}{\gamma_g}\left(-\chi_0 - \frac{2}{\omega}\frac{\gamma_0}{\gamma_g}\lambda_g + \beta\frac{\gamma_0}{\gamma_g}\right)\right\}^{-1} \delta(\lambda_g - \lambda_g^*). \quad (1)$$

In the amorphous medium, the field consists of the electron Coulomb field and the field of the emitted free photons $E_a^{(s)}$:

$$E_0^{(s)\mathrm{sr}} = \frac{8\pi^2 eiV\theta P^{(s)}}{\omega} \times \left\{\frac{\gamma_0}{\gamma_g}\left(-\chi_0 + \chi_a - \frac{2}{\omega}\frac{\gamma_0}{\gamma_g}\lambda_g + \beta\frac{\gamma_0}{\gamma_g}\right)\right\}^{-1} \times \delta(\lambda_g - \lambda_g^*) + E_a^{(s)}\delta(\lambda_g - \lambda_g'). \quad (2)$$

In the crystal, the field of the incident and diffracted waves consists of the relativistic-electron Coulomb

field and the fields of two freely propagating X-ray waves in the crystal:

$$E_0^{(s)\mathrm{cr}} = \frac{8\pi^2 ieV\theta P^{(s)}}{\omega}$$

$$\times \frac{-\omega^2\beta - 2\omega\dfrac{\gamma_g}{\gamma_0}\lambda_0}{4\dfrac{\gamma_g}{\gamma_0}(\lambda_0-\lambda_0^{(1)})(\lambda_0-\lambda_0^{(2)})}\delta(\lambda_0-\lambda_0^*) \qquad (3)$$

$$+ E_0^{(s)(1)}\delta(\lambda_0-\lambda_0^{(1)}) + E_0^{(s)(2)}\delta(\lambda_0-\lambda_0^{(2)}),$$

$$E_g^{(s)\mathrm{cr}} = -\frac{8\pi^2 ieV\theta P^{(s)}}{\omega}$$

$$\times \frac{\omega^2\chi_g C^{(s)}}{4\dfrac{\gamma_0^2}{\gamma_g^2}(\lambda_g-\lambda_g^{(1)})(\lambda_g-\lambda_g^{(2)})}\delta(\lambda_g-\lambda_g^*) \qquad (4)$$

$$+ E_g^{(s)(1)}\delta(\lambda_g-\lambda_g^{(1)}) + E_g^{(s)(2)}\delta(\lambda_g-\lambda_g^{(2)}).$$

It should be noted that the incident and diffracted fields in the crystal are related by the relation

$$E_0^{(s)\mathrm{cr}} = \frac{2\omega\lambda_g}{\omega^2\chi_g C^{(s)}}E_g^{(s)\mathrm{cr}}. \qquad (5)$$

The emitted field in a vacuum behind the target in the Bragg scattering direction will be

$$E_g^{(s)\mathrm{vacII}} = E_g^{(s)\mathrm{Rad}}\delta\left(\lambda_g + \omega\frac{\chi_0}{2}\right). \qquad (6)$$

Notation similar to that in [25, 27] is used in Eqs. (1)–(4):

$$\lambda_g^{(1,2)} = \frac{\omega|\chi_g'|C^{(s)}}{2}\left\{\xi^{(s)} - \frac{i\rho^{(s)}(1-\varepsilon)}{2}\right.$$

$$\pm\left(\xi^{(s)^2} + \varepsilon - 2i\rho^{(s)}\left(\frac{1-\varepsilon}{2}\xi^{(s)} + \kappa^{(s)}\varepsilon\right)\right.$$

$$\left.\left.-\rho^{(s)^2}\left(\frac{(1-\varepsilon)^2}{4} + \kappa^{(s)^2}\varepsilon\right)\right)^{1/2}\right\}, \qquad (7)$$

$$\lambda_g^* = \frac{\omega\beta}{2} + \frac{\gamma_g}{\gamma_0}\lambda_0^*, \quad \lambda_0^* = \omega\frac{\gamma^{-2} + \theta^2 - \chi_0}{2},$$

$$\lambda_g' = \lambda_g^* - \frac{\gamma_g}{\gamma_0}\omega\frac{\gamma^{-2} + \theta^2 - \chi_a}{2},$$

where $\gamma_0 = \cos\psi_0$, $\gamma_g = \cos\psi_g$, ψ_0 is the angle between the wave vector of the incident wave $\mathbf{k}$ and the normal vector $\mathbf{n}$ to the crystal-plate surface, ψ_g is the angle between the wave vector $\mathbf{k}_g$ and the normal vector $\mathbf{n}$ (see Fig. 1),

$$\xi^{(s)}(\omega) = \eta^{(s)}(\omega) + \frac{1-\varepsilon}{2\nu^{(s)}},$$

$$\eta^{(s)}(\omega) = \frac{2\sin^2\theta_B}{V^2|\chi_g'|C^{(s)}}$$

$$\times\left(1 - \frac{\omega(1-\theta\cos\varphi\cot\theta_B)}{\omega_B}\right),$$

$$\varepsilon = \frac{\gamma_g}{\gamma_0} = \frac{\cos\psi_g}{\cos\psi_0}, \quad \rho^{(s)} = \frac{\chi_0''}{|\chi_g'|C^{(s)}}, \qquad (8)$$

$$\kappa^{(s)} = \frac{\chi_g'' C^{(s)}}{\chi_0''}, \quad \nu^{(s)} = \frac{\chi_g' C^{(s)}}{\chi_0'},$$

$$C^{(1)} = 1, \quad C^{(2)} = \cos 2\theta_B,$$

$$P^{(1)} = \sin\varphi, \quad P^{(2)} = \cos\varphi.$$

Equations (1)–(6) with $s = 1$ and 2 describe the σ- and π-polarized fields, respectively. The dynamic addends $\lambda_g^{(1,2)}$ entering into the length of the wave vector $k_g = \omega\sqrt{1+\chi_0} + \lambda_g$ are small and, hence, it can be shown that $\theta \approx \theta'$ (see Fig. 1). Therefore, below we will designate the angle θ' as θ.

Since the inequality

$$2\sin^2\theta_B/V^2|\chi_g'|C^{(s)} \gg 1$$

holds in the X-ray frequency range, $\eta^{(s)}(\omega)$ is a fast function of frequency ω. Therefore, for the subsequent analysis of the PXR and DTR spectra, it is very convenient to consider $\eta^{(s)}(\omega)$ as a spectral variable characterizing the frequency ω.

An important parameter in Eq. (7) is ε, which can be represented as

$$\varepsilon = \frac{\sin(\delta+\theta_B)}{\sin(\delta-\theta_B)}.$$

It determines the degree of field reflection asymmetry in the crystal plate relative to the target surface. Here, θ_B is the angle between the electron velocity and the system of parallel atomic planes in the crystal, δ is the angle between the target surface and the reflecting planes. Note that the angle of incidence of the electron on the target surface, $\delta - \theta_B$, increases with decreasing parameter ε. The wave vectors of the incident and diffracted photons make equal and unequal angles with the plate surface in the cases of symmetric and asymmetric reflection, respectively; $\varepsilon = 1$ and $\delta = \pi/2$ in the symmetric case and $\varepsilon \neq 1$ and $\delta \neq \pi/2$ in the asymmetric one.

To determine the amplitude of the radiation field $E_g^{(s)\mathrm{Rad}}$, we will use the boundary conditions at the

three boundaries of the combined target under consideration:

$$\begin{aligned}
&\int E_0^{(s)\mathrm{vacI}} d\lambda_g = \int E_0^{(s)\mathrm{sr}} d\lambda_g,\\
&\int E_0^{(s)\mathrm{sr}} \exp\left(i\frac{\lambda_g}{\gamma_g}a\right) d\lambda_g\\
&= \int E_0^{(s)\mathrm{cr}} \exp\left(i\frac{\lambda_g}{\gamma_g}a\right) d\lambda_g,\\
&\int E_g^{(s)\mathrm{cr}} \exp\left(i\frac{\lambda_g}{\gamma_g}a\right) d\lambda_g = 0,\\
&\int E_g^{(s)\mathrm{cr}} \exp\left(i\frac{\lambda_g}{\gamma_g}(a+b)\right) d\lambda_g\\
&= \int E_g^{(s)\mathrm{vacII}} \exp\left(i\frac{\lambda_g}{\gamma_g}(a+b)\right) d\lambda_g.
\end{aligned} \tag{9}$$

In this paper, we restrict our analysis of the radiation from a relativistic electron in the combined medium to rectilinear electron motion. Therefore, only two radiation mechanisms contribute to the total radiation yield: PXR and DTR. We will represent the amplitude of the coherent radiation field $E_g^{(s)\mathrm{Rad}}$ as the sum of two terms:

$$E_g^{(s)\mathrm{Rad}} = E_{\mathrm{PXR}}^{(s)} + E_{\mathrm{DTR}}^{(s)}, \tag{10a}$$

$$\begin{aligned}
E_{\mathrm{PXR}}^{(s)} = {} & \frac{8\pi^2 ieV\theta P^{(s)}}{\omega} \exp\left\{i\left(\frac{\omega\chi_0}{2} + \lambda_g^*\right)\frac{a+b}{\gamma_g}\right\}\\
& \times \frac{\omega^2 \chi_g C^{(s)}}{2\omega\frac{\gamma_0}{\gamma_g}(\lambda_g^{(1)} - \lambda_g^{(2)})}\\
& \times \left[\left(\frac{1}{\chi_0 - \theta^2 - \gamma^{-2}} + \frac{\omega}{2\frac{\gamma_0}{\gamma_g}(\lambda_g^* - \lambda_g^{(1)})}\right)\right.\\
& \times \left(\exp\left\{i\frac{\lambda_g^{(1)} - \lambda_g^*}{\gamma_g}b\right\} - 1\right)\\
& - \left(\frac{1}{\chi_0 - \theta^2 - \gamma^{-2}} + \frac{\omega}{2\frac{\gamma_0}{\gamma_g}(\lambda_g^* - \lambda_g^{(2)})}\right)\\
& \left.\times \left(\exp\left\{i\frac{\lambda_g^{(2)} - \lambda_g^*}{\gamma_g}b\right\} - 1\right)\right],
\end{aligned} \tag{10b}$$

$$\begin{aligned}
E_{\mathrm{DTR}}^{(s)} = {} & \frac{8\pi^2 ieV\theta P^{(s)}}{\omega} \exp\left\{i\left(\frac{\omega\chi_0}{2} + \lambda_g^*\right)\frac{a+b}{\gamma_g}\right\} \frac{\omega^2 \chi_g C^{(s)}\left(\exp\left\{i\frac{\lambda_g^{(1)} - \lambda_g^*}{\gamma_g}b\right\} - \exp\left\{i\frac{\lambda_g^{(2)} - \lambda_g^*}{\gamma_g}b\right\}\right)}{2\omega\frac{\gamma_0}{\gamma_g}(\lambda_g^{(1)} - \lambda_g^{(2)})}\\
& \times \left[\left(\frac{1}{\theta^2 + \gamma^{-2} - \chi_a} - \frac{1}{\theta^2 + \gamma^{-2}}\right)\exp\left\{-i\frac{\omega a}{2\gamma_0}(\theta^2 + \gamma^{-2} - \chi_a)\right\} + \left(\frac{1}{\chi_a - \theta^2 - \gamma^{-2}} - \frac{1}{\chi_0 - \theta^2 - \gamma^{-2}}\right)\right].
\end{aligned} \tag{10c}$$

Equation (10b) represents the field amplitude of PXR from a relativistic electron in the combined medium produced when the electron crosses the crystal plate located behind the amorphous one. The terms in square brackets correspond to the two PXR waves excited in the crystal medium in the Bragg scattering direction. At least one of the following equalities should hold for the PXR reflection to arise:

$$\mathrm{Re}(\lambda_g^* - \lambda_g^{(1)}) = 0, \quad \mathrm{Re}(\lambda_g^* - \lambda_g^{(2)}) = 0,$$

i.e., the real part of the denominator of at least one of the terms in square brackets in Eq. (10b) should be zero.

Equation (10c) describes the amplitude of the diffracted transition radiation in the combined structure that includes the transition radiation arisen at the first and second boundaries and then diffracted by a system of parallel atomic planes in the crystal plate. The first term in square brackets in Eq. (10c) refers to the transition radiation arising when a relativistic electron crosses the vacuum–amorphous medium boundary and the second term refers to the transition radiation excited at the second boundary (between the amorphous medium and the crystal). Since the expressions for the PXR and DTR field amplitudes were derived from the total field amplitude of the coherent radiation, they allow the influence of the interference between PXR and DTR and the interference between the transition radiations arisen at different boundaries of the combined medium on the resultant radiation from the target to be investigated.

3. THE SPECTRAL-ANGULAR RADIATION DENSITY

Substituting (10b) and (10c) into the well-known [28] expression for the spectral-angular density of X-ray radiation,

$$\omega\frac{d^2N}{d\omega d\Omega} = \omega^2(2\pi)^{-6}\sum_{s=1}^{2}\left|E_g^{(s)\mathrm{Rad}}\right|^2, \tag{11}$$

we will obtain the expressions describing the spectral-angular PXR and DTR densities for a relativistic electron in the combined amorphous–crystal medium:

$$\omega\frac{d^2N_{\mathrm{PXR}}^{(s)}}{d\omega d\Omega} = \frac{e^2}{4\pi^2}P^{(s)^2} \times \frac{\theta^2}{\left(\theta^2+\gamma^{-2}-\chi_0'\right)^2}R_{\mathrm{PXR}}^{(s)}, \tag{12a}$$

$$R_{\mathrm{PXR}}^{(s)} = \left(1-\frac{\xi^{(s)}}{\sqrt{\xi^{(s)^2}+\varepsilon}}\right)^2 \times \frac{1+\exp(-2B^{(s)}\rho^{(s)}\Delta^{(1)})-2\exp(-B^{(s)}\rho^{(s)}\Delta^{(1)})\cos\left(B^{(s)}\left(\sigma^{(s)}+\frac{\xi^{(s)}-\sqrt{\xi^{(s)^2}+\varepsilon}}{\varepsilon}\right)\right)}{\left(\sigma^{(s)}+\frac{\xi^{(s)}-\sqrt{\xi^{(s)^2}+\varepsilon}}{\varepsilon}\right)^2+\rho^{(s)^2}\Delta^{(1)^2}}, \tag{12b}$$

$$\omega\frac{d^2N_{\mathrm{DTR}}^{(s)}}{d\omega d\Omega} = \frac{e^2}{4\pi^2}P^{(s)^2}G(\theta)R_{\mathrm{DTR}}^{(s)}, \tag{13a}$$

$$G(\theta) = \theta^2\left(\frac{1}{\theta^2+\gamma^{-2}}-\frac{1}{\theta^2+\gamma^{-2}-\chi_a'}\right)^2 \times \exp\left(-\frac{\omega\chi_a''}{\gamma_0}a\right) + \theta^2\left(\frac{1}{\theta^2+\gamma^{-2}-\chi_a'}-\frac{1}{\theta^2+\gamma^{-2}-\chi_a'}\right)^2 + 2\theta^2\left(\frac{1}{\theta^2+\gamma^{-2}}-\frac{1}{\theta^2+\gamma^{-2}-\chi_a'}\right) \times \left(\frac{1}{\theta^2+\gamma^{-2}-\chi_a'}-\frac{1}{\theta^2+\gamma^{-2}-\chi_0'}\right) \times \cos\left(\frac{\omega a}{2\gamma_0}(\theta^2+\gamma^{-2}-\chi_a')\right)\exp\left(-\frac{\omega\chi_a''}{2\gamma_0}a\right), \tag{13b}$$

$$R_{\mathrm{DTR}}^{(s)} = \frac{\varepsilon^2}{\xi(\omega)^2+\varepsilon}\left[\exp(-2B^{(s)}\rho^{(s)}\Delta^{(1)}) + \exp(-2B^{(s)}\rho^{(s)}\Delta^{(2)})-2\exp\left(-B^{(s)}\rho^{(s)}\frac{1+\varepsilon}{\varepsilon}\right) \times \cos\frac{2B^{(s)}\sqrt{\xi^{(s)^2}+\varepsilon}}{\varepsilon}\right], \tag{13c}$$

where

$$\Delta^{(2)} = \frac{\varepsilon+1}{2\varepsilon}+\frac{1-\varepsilon}{2\varepsilon}\frac{\xi^{(s)}}{\sqrt{\xi^{(s)^2}+\varepsilon}}+\frac{\kappa^{(s)}}{\sqrt{\xi^{(s)^2}+\varepsilon}},$$

$$\Delta^{(1)} = \frac{\varepsilon+1}{2\varepsilon}-\frac{1-\varepsilon}{2\varepsilon}\frac{\xi^{(s)}}{\sqrt{\xi^{(s)^2}+\varepsilon}}-\frac{\kappa^{(s)}}{\sqrt{\xi^{(s)^2}+\varepsilon}},$$

$$\sigma^{(s)} = \frac{1}{\nu^{(s)}}\left(\frac{\theta^2}{|\chi_0'|}+\frac{1}{\gamma^2|\chi_0'|}+1\right), \tag{14}$$

$$B^{(s)} = \frac{\omega|\chi_g'|C^{(s)}}{2}\frac{b}{\gamma_0}, \quad \varepsilon = \frac{\sin(\delta+\theta_{\mathrm{B}})}{\sin(\delta-\theta_{\mathrm{B}})}.$$

The parameter $B^{(s)}$ can be represented as

$$B^{(s)} = \frac{1}{2\sin(\delta-\theta_{\mathrm{B}})}\frac{b}{L_{\mathrm{ext}}^{(s)}}. \tag{15}$$

It can be seen from Eq. (15) that patameter $B^{(s)}$ is equal to half the electron path in the crystal plate expressed in X-ray extinction lengths in the crystal $L_{\mathrm{ext}}^{(s)} = (\omega|\chi_g'|C^{(s)})^{-1}$.

The PXR yield is formed mainly only by one of the branches corresponding to the second term in (10b). As is easy to verify directly, only in this term does the real part of the denominator become zero. The solution of the corresponding equation,

$$\sigma^{(s)}+\frac{\xi^{(s)}-\sqrt{\xi^{(s)^2}+\varepsilon}}{\varepsilon} = 0, \tag{16}$$

defines the frequency ω_* near which the spectrum of the PXR photons emitted at a fixed observation angle is concentrated.

The functions $R^{(s)}_{\mathrm{PXR}}$ and $R^{(s)}_{\mathrm{DTR}}$ in the derived equations (12) and (13) represent the PXR and DTR spectra that describe the passage of free and coupled X-ray photons, respectively, through the crystal plate within the dynamic diffraction theory. It should be noted that the two X-ray waves excited in the crystal with the linear absorption coefficients

$$\begin{aligned}\mu_1^{(s)} &= \omega\chi_0''\varepsilon\Delta^{(1)} \equiv \frac{\varepsilon}{L_{\mathrm{ext}}}\rho^{(s)}\Delta^{(1)},\\ \mu_2^{(s)} &= \omega\chi_0''\varepsilon\Delta^{(2)} \equiv \frac{\varepsilon}{L_{\mathrm{ext}}}\rho^{(s)}\Delta^{(2)},\end{aligned} \tag{17}$$

contribute to the DTR spectrum, while only one wave with the absorption coefficient $\mu_1^{(s)}$ contributes to the PXR spectrum.

The function $G(\theta)$ in Eq. (13b) describes the angular dependence of the diffracted transition radiation and consists of three terms. The first term corresponds to the transition radiation arising when a relativistic electron crosses the first boundary, which subsequently passes through the amorphous medium and is diffracted in the crystal plate in the Bragg direction. The second term corresponds to the transition radiation arising at the second boundary (between the amorphous medium and the crystal) and also diffracted in the crystal plate in the direction of Bragg reflection. The third term describes the interference between these two DTR waves.

Equations (12) and (13) derived within the dynamic diffraction theory, which describe the spectral-angular distributions of PXR and DTR from a relativistic electron in the combined medium, are the main result of this paper. These expressions take into account the field reflection asymmetry (parameter ε) in the crystal plate relative to the target surface.

4. A THIN NONABSORBING TARGET

Consider the radiation properties for the comparatively simple case of a thin target where the absorption coefficients can be neglected, i.e., we can set $\rho^{(s)} = 0$. In this case, the spectral-angular distributions of the PXR and DTR yields following from (12) and (13) transform into the expressions

$$\omega\frac{d^2N^{(s)}_{\mathrm{PXR}}}{d\omega d\Omega} = \frac{e^2}{4\pi^2}\frac{P^{(s)^2}}{|\chi_0'|}T^{(s)}_{\mathrm{PXR}}, \tag{18a}$$

$$T^{(s)}_{\mathrm{PXR}} = \frac{\theta^2}{|\chi_0'|}\frac{1}{(\Gamma+1)^2}R^{(s)}_{\mathrm{PXR}}, \tag{18b}$$

$$\begin{aligned}R^{(s)}_{\mathrm{PXR}} &= 4\left(1-\frac{\xi}{\sqrt{\xi^2+\varepsilon}}\right)^2\\ &\times\frac{\sin^2\left(\frac{B^{(s)}}{2}\left(\sigma^{(s)}+\frac{\xi-\sqrt{\xi^2+\varepsilon}}{\varepsilon}\right)\right)}{\left(\sigma^{(s)}+\frac{\xi-\sqrt{\xi^2+\varepsilon}}{\varepsilon}\right)^2},\end{aligned} \tag{18c}$$

$$\omega\frac{d^2N^{(s)}_{\mathrm{DTR}}}{d\omega d\Omega} = \frac{e^2}{4\pi^2}\frac{P^{(s)^2}}{|\chi_0'|}T^{(s)}_{\mathrm{DTR}}, \tag{19a}$$

$$T^{(s)}_{\mathrm{DTR}} = T^{1(s)}_{\mathrm{DTR}} + T^{2(s)}_{\mathrm{DTR}} + T^{\mathrm{int}(s)}_{\mathrm{DTR}}, \tag{19b}$$

$$T^{1(s)}_{\mathrm{DTR}} = \frac{\theta^2}{|\chi_0'|}\left(\frac{1}{\Gamma}-\frac{1}{\Gamma_a}\right)^2 R^{(s)}_{\mathrm{DTR}}, \tag{19c}$$

$$T^{2(s)}_{\mathrm{DTR}} = \frac{\theta^2}{|\chi_0'|}\left(\frac{1}{\Gamma_a}-\frac{1}{\Gamma+1}\right)^2 R^{(s)}_{\mathrm{DTR}}, \tag{19d}$$

$$\begin{aligned}T^{\mathrm{int}(s)}_{\mathrm{DTR}} &= 2\frac{\theta^2}{|\chi_0'|}\left(\frac{1}{\Gamma}-\frac{1}{\Gamma_a}\right)\left(\frac{1}{\Gamma_a}-\frac{1}{\Gamma+1}\right)\\ &\times\cos\left(B^{(s)}\frac{a}{b}\frac{1}{\nu^{(s)}}\Gamma_a\right)R^{(s)}_{\mathrm{DTR}},\end{aligned} \tag{19e}$$

$$R^{(s)}_{\mathrm{DTR}} = \frac{4\varepsilon^2}{\xi^2+\varepsilon}\sin^2\frac{B^{(s)}\sqrt{\xi^2+\varepsilon}}{\varepsilon}, \tag{19f}$$

where

$$\Gamma = \frac{\theta^2}{|\chi_0'|}+\frac{1}{\gamma^2|\chi_0'|}, \quad \Gamma_a = \frac{\theta^2}{|\chi_0'|}+\frac{1}{\gamma^2|\chi_0'|}+\frac{\chi_a'}{\chi_0'}.$$

The quantity $T^{(s)}_{\mathrm{DTR}}$ in Eq. (19b) is represented as the sum of the terms describing the diffracted radiations from the first and second boundaries, respectively, $T^{1(s)}_{\mathrm{DTR}}$ and $T^{2(s)}_{\mathrm{DTR}}$ and their interference term $T^{\mathrm{int}(s)}_{\mathrm{DTR}}$.

When passing from Eqs. (13) to Eqs. (19), we used the obvious relation

$$\begin{aligned}&\frac{\omega a}{2\gamma_0}(\theta^2+\gamma^{-2}-\chi_a')\\ &= B^{(s)}\frac{a}{b}\frac{1}{\nu^{(s)}}\left(\frac{\theta^2}{|\chi_0'|}+\frac{1}{\gamma^2|\chi_0'|}+\frac{\chi_a'}{\chi_0'}\right),\end{aligned} \tag{20}$$

where the parameters of the first amorphous layer are expressed in terms of the parameters of the crystal layer and the ratios of the parameters of both layers: a/b and χ_a'/χ_0'. Instead of the observation angle θ, it is more convenient to use the observation angle normalized to $\sqrt{|\chi_0'|}$, i.e., the parameter $\theta/\sqrt{|\chi_0'|}$. Note that the dielectric susceptibility in the X-ray frequency

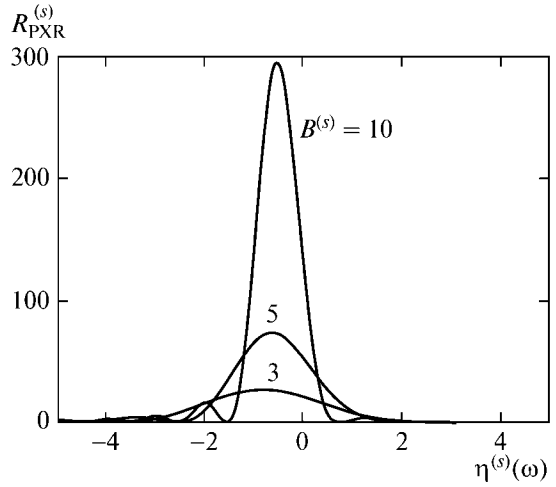

Fig. 2. PXR spectra for various crystal-plate thicknesses at $\varepsilon = 3$, $\theta/\sqrt{|\chi_0'|} = 0.3$, $1/\gamma\sqrt{|\chi_0'|} = 0.3$, and $\nu^{(s)} = 8$.

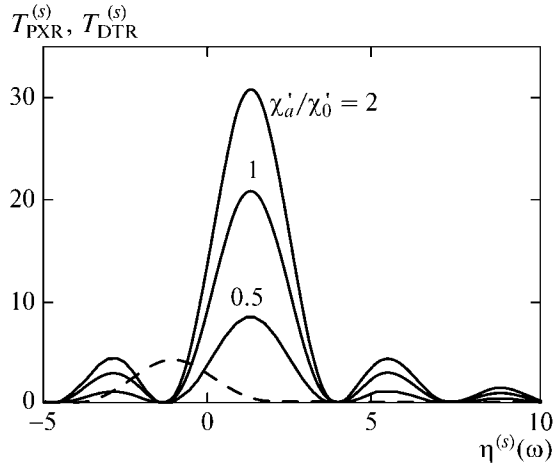

Fig. 3. PXR (dashed curve) and DTR (solid curves) spectra for various amorphous media (various ratios χ_a'/χ_0') at $B^{(s)} = 3$, $a/b = 1$, $\varepsilon = 3$, $\theta/\sqrt{|\chi_0'|} = 0.5$, $1/\gamma\sqrt{|\chi_0'|} = 0.2$, and $\nu^{(s)} = 0.8$.

range under consideration is described by the expression

$$\chi_a = \chi_a' + i\chi_a'',$$

where

$$\chi_a' = -\frac{\omega_0^2}{\omega^2}, \quad \omega_a^2 = \frac{4\pi Z_a e^2 n_a}{m},$$

Z_a is the number of electrons in the atom, and n_a is the density of atoms. Hence it follows that

$$\frac{\chi_a'}{\chi_0'} = \frac{Z_a n_a}{Z_0 n_0},$$

i.e., the ratio of the real parts of the dielectric susceptibilities for the amorphous and crystal parts of the target is proportional to the ratio of the densities of their materials.

Consider the PXR spectrum of a relativistic electron crossing the combined medium that is described by the function $R^{(s)}_{PXR}$ (see (18c)). It can be seen that the spectrum depends on the thickness of the crystal component of the target and does not depend on the thickness of the amorphous one. This spectrum can be observed at a fixed observation angle θ. The curves describing the PXR spectrum that were constructed from Eq. (18c) are presented in Fig. 2. These curves show the growth of the spectrum amplitude with increasing thickness of the crystal target b entering into the parameter $B^{(s)}$. The curves presented in Fig. 2, along with all those considered below, were constructed for the specific reflection asymmetry parameter $\varepsilon = 3$ defining the angle δ between the system of parallel atomic planes in the crystal and the target surface at a fixed angle θ_B.

Next, consider the influence of dielectric amorphous-target properties on the diffracted transition radiation. Figure 3 presents the curves of the spectral-angular PXR and DTR densities constructed from Eqs. (18b) and (19b) at fixed observation angle θ, electron Lorentz factor γ, and crystal-plate parameters. The thickness of the amorphous and crystal plates was chosen to be the same, $a/b = 1$. It follows from the fig-

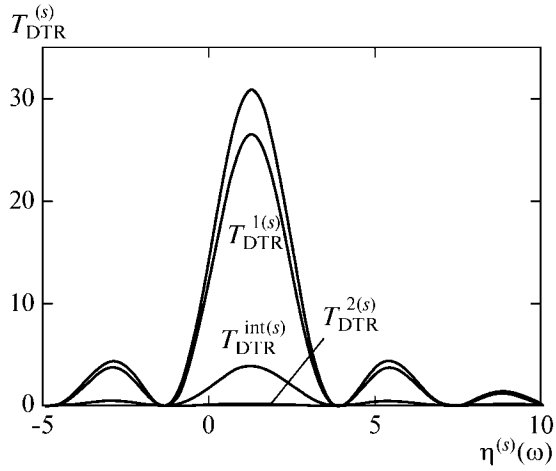

Fig. 4. Contributions from the transition radiation waves excited at the first and second boundaries and their interference term to the DTR spectrum at $\chi_a'/\chi_0' = 2$. The parameters are the same as those in Fig. 3.

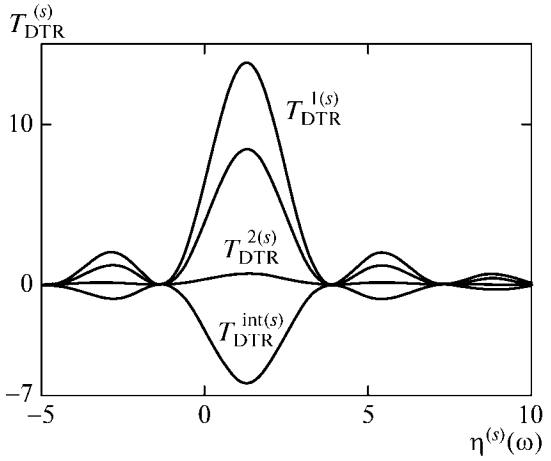

Fig. 5. Same as Fig. 4 for $\chi_a'/\chi_0' = 0.5$.

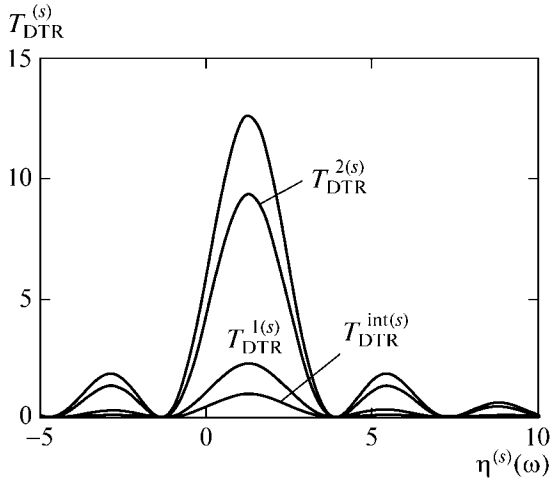

Fig. 6. Same as Fig. 5 for $\chi_a'/\chi_0' = 0.1$.

ure that the DTR density increases significantly with increasing ratio

$$\frac{\chi_a'}{\chi_0'} = \frac{Z_a n_a}{Z_0 n_0},$$

i.e., with increasing density of the material of the amorphous medium. At the same time, the spectral-angular PXR density does not change. Thus, the spectral-angular DTR density can be increased by changing the material of the amorphous medium without increasing the electron energy, while the formulas derived here allow the spectral-angular DTR and PXR densities as a function of target parameters to be calculated.

The contributions from the transition radiations produced at the first and second boundaries of the combined medium and their interference term to the spectral-angular DTR density are shown by the curves constructed from Eqs. (19b), (19c), (19d), and (19e) and presented in Figs. 4–6. It can be seen from Fig. 4 that in the case where the amorphous medium is denser than the crystal one, the wave excited at the first boundary makes a major contribution to the DTR yield. In this case, the interference term turns out to be more significant than the term defining the contribution from the wave excited at the second boundary of the combined medium. As the density of the amorphous medium decreases, the interference term can make a destructive contribution to the spectral-angular DTR density (see Fig. 5). If, however, the density of the amorphous medium is decreased significantly, then the contribution from the transition radiation wave excited at the second boundary to the total DTR can become overwhelming. We can arrive at all these conclusions directly by analytically analyzing Eqs. (19). Note that, as follows from (19), a change in the thickness of the amorphous medium a in the case of a thin nonabsorbing target affects only the interference term and cannot affect significantly the spectral density.

Consider the influence of the amorphous medium on the angular DTR density via the parameter χ_a'/χ_0'. For this purpose, let us integrate Eqs. (18a) and (19a) over the frequency function $\eta^{(s)}(\omega)$:

$$\frac{dN_{PXR}^{(s)}}{d\Omega} = \frac{e^2 P^{(s)^2}}{8\pi^2 \sin^2\theta_B} F_{PXR}^{(s)}(\theta), \tag{21a}$$

$$F_{PXR}^{(s)}(\theta) = \nu^{(s)} \int_{-\infty}^{\infty} T_{PXR}^{(s)} d\eta^{(s)}(\omega), \tag{21b}$$

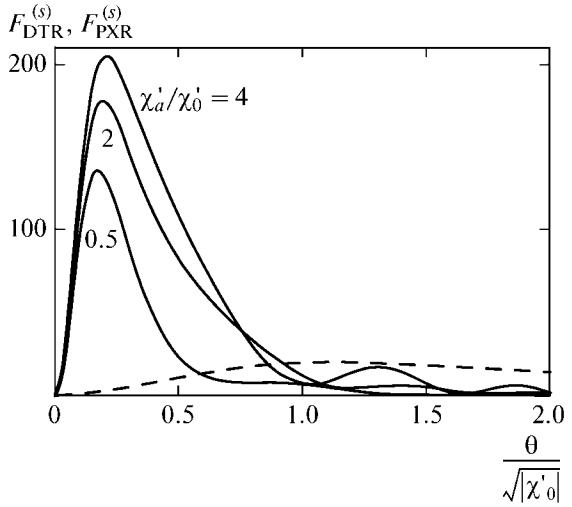

Fig. 7. Angular PXR (dashed curve) and DTR (solid curves) densities for various amorphous media at $B^{(s)} = 3$, $a/b = 1$, $\varepsilon = 3$, $1/\gamma\sqrt{|\chi_0'|} = 0.2$, and $\nu^{(s)} = 0.8$.

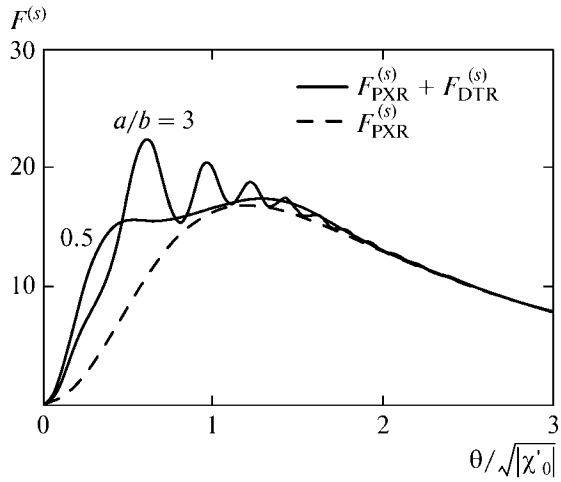

Fig. 8. Influence of the transition radiation from the amorphous substrate on the angular PXR density for various ratios a/b at $\chi'_a/\chi'_0 = 0.5$, $B^{(s)} = 3$, $\varepsilon = 3$, $1/\gamma\sqrt{|\chi'_0|} = 0.5$, and $\nu^{(s)} = 0.8$.

$$\frac{dN^{(s)}_{DTR}}{d\Omega} = \frac{e^2 P^{(s)^2}}{8\pi^2 \sin^2\theta_B} F^{(s)}_{DTR}(\theta), \qquad (21c)$$

$$F^{(s)}_{DTR}(\theta) = \nu^{(s)} \int_{-\infty}^{\infty} T^{(s)}_{DTR} d\eta^{(s)}(\omega). \qquad (21d)$$

The curves describing the angular DTR and PXR densities are constructed in Fig. 7. It follows from these curves that, just as for the spectral-angular density, an increase in the ratio χ'_a/χ'_0 at a fixed observational angle (see Fig. 3) causes the angular DTR density to increase significantly. This fact can be used in producing compact, intense alternative X-ray radiation sources based on the interaction of relativistic electrons with complex structured materials.

As the energy of the radiating electrons decreases, the PXR contribution to the total angular density becomes decisive, but DTR can lead to various deformations or oscillations in the angular density of the total coherent radiation (see Fig. 8) depending on the ratio a/b defining the amorphous-plate thickness at a fixed crystal-plate thickness b. Thus, the formulas describing the spectral-angular PXR and DTR densities derived here can be used in interpreting the data from experiments in which an amorphous medium acts as the substrate of a thin crystal plate.

5. CONCLUSIONS

We developed a theory of coherent X-ray radiation from a relativistic electron crossing a combined medium consisting of amorphous and crystal plates within the dynamic diffraction theory. Based on the two-wave approximation of the dynamic diffraction theory, we derived the expressions describing the spectral-angular densities of parametric X-ray and diffracted transition radiations. Our calculations of the spectral-angular distributions based on these expressions allowed us to show that the DTR contribution to the total radiation from the combined target increases with increasing ratio of the density of the amorphous medium to the density of the crystal one, while the PXR contribution does not change. We investigated the contribution from the transition radiation waves generated at the first and second boundaries and their interference term to the total DTR yield. We investigated the influence of the transition radiation from the amorphous substrate diffracted by a system of parallel atomic planes in the crystal part of the target on the spectral-angular characteristics of the coherent X-ray radiation from the combined target.

REFERENCES

1. V. L. Ginzburg and I. M. Frank, Zh. Eksp. Teor. Fiz. **16**, 15 (1946); V. Ginzburg and I. Frank, J. Phys. (USSR) **9**, 353 (1945).
2. V. L. Ginzburg and V. N. Tsytovich, *Transition Radiation and Transition Scattering* (Nauka, Moscow, 1984; Adam Hilger, Bristol, 1990).
3. A. V. Kol'tsov and A. V. Serov, J. Exp. Theor. Phys. **116** (5), 732 (2013).
4. A. V. Serov and B. M. Bolotovskii, J. Exp. Theor. Phys. **104** (6), 866 (2007).
5. M. I. Ryazanov, J. Exp. Theor. Phys. **98** (3), 478 (2004).
6. A. P. Potylitsyn and R. O. Rezaev, Nucl. Instrum. Methods Phys. Res., Sect. B **252**, 44 (2006).
7. D. Yu. Sergeeva, A. A. Tishchenko, and M. N. Strikhanov, Nucl. Instr. Meth. Phys. Res., Sect. B **309**, 189 (2013).
8. N. F. Shul'ga and V. V. Syshchenko, Nucl. Instrum. Method Phys. Res., Sect. B **201**, 78 (2003).
9. R. Rullhusen, X. Artru, and P. Dhez, *Novel Radiation Sources Using Relativistic Electrons* (World Scientific, Singapore, 1999).
10. A. Caticha, Phys. Rev. A: At., Mol., Opt. Phys. **40**, 4322 (1989).
11. V. Baryshevsky, Nucl. Instrum. Methods Phys. Res., Sect. A **122**, 13 (1997).
12. X. Artru and P. Rullhusen, Nucl. Instrum. Methods Phys. Res., Sect. B **145**, 1 (1998).
13. N. Nasonov, Phys. Lett. A **246**, 148 (1998).
14. M. L. Ter-Mikaelyan, *High-Energy Electromagnetic Processes in Condensed Media* (Academy of Sciences of Armenian SSR, Yerevan, 1969; Wiley, New York, United States, 1972).
15. G. M. Garibyan and Yan Shi, Sov. Phys. JETP **34**, 495 (1971).
16. V. G. Baryshevskii and I. D. Feranchuk, Sov. Phys. JETP **34**, 502 (1971).
17. H. Nitta, Phys. Lett. A **158**, 270 (1991).

18. I. D. Feranchuk and A. V. Ivashin, J. Phys. (Paris) **46**, 1981 (1985).
19. V. G. Baryshevsky and I. D. Feranchuk, J. Phys. (Paris) **44**, 913 (1983).
20. N. Nasonov, Phys. Lett. A **292**, 146 (2001).
21. N. Nasonov and A. Noskov, Nucl. Instrum. Methods Phys. Res., Sect. B **201**, 67 (2003).
22. N. N. Nasonov, P. Zhukova, M. A. Piestrup, and H. Park, Nucl. Instrum. Methods Phys. Res., Sect. B **251**, 96 (2006).
23. S. Blazhevich and A. Noskov, Nucl. Instrum. Methods Phys. Res., Sect. B **252**, 69 (2006).
24. S. V. Blazhevich and A. V. Noskov, Nucl. Instrum. Methods Phys. Res., Sect. B **266**, 3770 (2008).
25. S. V. Blazhevich and A. V. Noskov, J. Exp. Theor. Phys. **109** (6), 901 (2009).
26. Z. G. Pinsker, *Dynamical Scattering of X-Rays in Crystals* (Nauka, Moscow, 1974; Springer-Verlag, Berlin, 1978).
27. S. V. Blazhevich, I. V. Kolosova, and A. V. Noskov, J. Surf. Invest. **6** (2), 348 (2012).
28. V. A. Bazylev and N. K. Zhevago, *Radiation of Fast Particles in Matter and External Fields* (Nauka, Moscow, 1987) [in Russian].

Translated by V. Astakhov